Nonlinear Robust Observer Design Using An Invariant Manifold Approach

Irfan Ullah Khan, David Wagg, Neil D Sims

Department of Mechanical Engineering, The University of Sheffield, Sheffield, UK

Abstract

This paper presents a method to design a reduced order observer using an invariant manifold approach. The main advantages of this method are that it enables a systematic design approach, and (unlike most nonlinear observer design methods), it can be generalized over a larger class of nonlinear systems. The method uses specific mapping functions in a way that minimises the error dynamics close to zero. Another important aspect is the robustness property which is due to the manifold attractivity: an important feature when an observer is used in a closed loop control system. A two degree-of-freedom system is used as an example. The observer design is validated using numerical simulation. Then experimental validation is carried out using hardware-in-the-loop testing. The proposed observer is then compared with a very well known nonlinear observer based on the off-line solution of the Riccati equation for systems with Lipschitz type nonlinearity. In all cases, the performance of the proposed observer is shown to be very high.

Keywords: observer design, invariant manifold, Lipschitz non-linearity, error dynamics, mapping functions

1. Introduction

For nonlinear systems the theory of linear observer design has been extended e.g. extended Luenburger observer [1, 2] or extended Kalman filter [3, 4]. As a result estimation is limited to a small domain and requires high computation power. In 1973 Thau [5] and then in 1975 Kou [6] were the first to attempt nonlinear techniques for the observer design. Since then a lot of work has been done on the observer design using nonlinear theory but mostly limited to certain classes of system that cannot typically be generalized to other classes of systems.

The observers based on Lyapunov theory give sufficient conditions for the existence of the observer for nonlinear systems [7, 8, 9]. It may be possible for the low order nonlinear systems to satisfy the conditions presented in the theorems based on Lyapunov theory but it is very difficult to find higher order nonlinear systems that can satisfy those conditions [10]. The observers based on extended linearization techniques linearize the error dynamics through a nonlinear output injection function [11, 12, 13]. This type of observer functions locally at a fixed point and for multi-input multi-output systems the design methodology can be very complicated.

For nonlinear observers, designs based on Lie-algebraic theory have also been used in the literature [10, 14, 15]. In these techniques, the problems linked with nonlinear observer design have been dealt with by using linear techniques

---

Email address: `(iukhan1, david.wagg, n.sims) @sheffield.ac.uk` (Irfan Ullah Khan, David Wagg, Neil D Sims)

that exploit linear observer theory. One of the advantages of using Lie-algebraic theory over the extended linearization techniques is that in the former case the observer is valid in any region where the transformation exists, whereas in the latter case the observer is designed at a fixed point. This method can also be used to design observer for multi-input multi-output systems. The down side of this technique is that the nonlinear system must satisfy both a non-generic condition along with the finding of a necessary state transformation, which is not an easy task.

Generally there are two ways to deal with observer design in nonlinear systems [16]. If the system nonlinearities are a linear function of unmeasured states or are monotonic, then observers based on linear theory can be used, or passivity can be exploited. Alternatively, the observer requires the existence of an attractive and invariant manifold. These types of observers comprise of a linear filter and nonlinear output mapping functions. The theory of sliding mode has also been used to design observers for both linear and nonlinear systems [17, 18].

The observer design in the sliding mode methodology resembles the one proposed in this paper up to the extent of defining an asymptotically stable surface. In the sliding mode observer, the sliding surface is defined in terms of the error between the estimated and known states and a discontinuous/switching function is defined to bring the error dynamics to the sliding surface [19, 20, 21], whereas in the proposed approach the observer design is reduced to make the error dynamics asymptotically stable, which depends on the definition of some mapping functions. The sliding mode observer is known for its insensitivity to parameter variation and disturbance rejection but the observer matching condition restricts the applicability of the sliding mode observer and the system has to be minimum phase [22, 23]. This means that all the zeros of the system should be on the left hand side, or in other words the internal dynamics of the system need to be stable for the design of first order sliding mode observer. To overcome this issue higher order sliding mode observers are proposed [24, 25]. However, the technique proposed in the present contribution could be extended, in a similar fashion for non-minimum phase systems [16].

Mainly there are two types of sliding mode observers. The type based on equivalent control methods are Utkin observers and the type based on Lyapunov methods are Walcott and Zak observers [26]. The Utkin sliding mode observer [27] does not have a static observer gain. The disadvantage of not having a static observer gain is that the state estimation can be performed only with the bounded error and not asymptotically. The Walcott and Zak observer has a static observer gain and the error is reduced based on system uncertainty. Another disadvantage of traditional sliding mode observers is high frequency switching action.

In [28, 29, 30, 31] the observer designs based on the solution of the Riccati equation are proposed for systems with Lipchitz type nonlinearity. In all these papers, to check the validity of the observer, the only test performed is that different initial conditions are given to the actual system and it is shown that the observer is converging. There is no discussion about the robustness of the observers against parameter variation, measurement noise or external disturbance. In this paper in addition to the initial condition test, both the proposed observer and the observer based on the off-line solution of the Riccati equation are tested for robustness against parameter variation, measurement noise and external disturbance.

The theory for observer developed by Astolfi *et al.* [16] , has been implemented on many systems, such as ball and

beam system, range estimation in a vision system and magnetic levitation system. The present contribution builds upon these previous studies by demonstrating application of the observer to a real mechanical system both in open loop and closed loop, so that the robustness to parameter variation, external disturbance and measurement noise, can be explored for the first time. Therefore, the idea presented by Astolfi *et al.* is further extended to systems with nonlinear stiffness. In this work a reduced order observer using the notion of an invariant manifold has been designed for a 2-DOF mass-spring-damper system to estimate the displacement and velocity of one of the masses. In addition a comparative study is presented with a very well known observer based on the off-line solution of the Riccati equation for systems with Lipschitz type nonlinearity.

The approach presented in this paper requires the existence of a manifold that is invariant and attractive [32, 33, 34, 35, 36]. The manifold is made invariant by a nonlinear filter and attractive by proper selection of mapping functions. To prove the validity of the proposed observer, it is compared with a very well known nonlinear observer based on Lipschitz type non-linearity presented in [37], which is based on the off-line solution of the Riccati equation. The reason for this comparison is that the system under consideration has a Lipschitz type nonlinearity. The result is that both observers show satisfactory results under normal conditions, but the proposed new observer is more robust to parameter variation and phase change in the excitation signal. Finally the proposed reduced order observer is tested in a closed loop with a hybrid active and semi-active controller to demonstrate the practical utility of the technique.

The details of the proposed observer design is given in Section 2. In Section 3 we introduce the example system that will be used throughout this paper. The proposed observer design is applied to the example system in Section 4. In Section 5 an observer based on Lipschitz type nonlinearity is designed for the same example system. Comparison results for both observers are given in Section 6. In Section 7 the experimental system is described and then the experimental results are presented, followed by further discussion in Section 8.

2. Proposed Observer Design Methodology

Consider a nonlinear, time-varying system described as

$$\dot{\eta} = f(\eta, y, t), \tag{1}$$

$$\dot{y} = h(\eta, y, t), \tag{2}$$

where $\eta \in \mathbb{R}^n$ is the unmeasured state, $y \in \mathbb{R}^m$ is the measurable output, an over-dot represents differentiation with respect to time, $f(\eta, y, t)$ and $h(\eta, y, t)$ are nonlinear functions. It is assumed that $f(\eta, y, t)$ and $h(\eta, y, t)$ are forward complete, *i.e.* trajectories starting at time t_0 are defined for all times $t \geq t_0$.

Let $\hat{\eta} \in \mathbb{R}^p$ represent the observer state, and $p \geq n$. From this, the total number of states of the system is $p + n$. Then the dynamical system

$$\dot{\hat{\eta}} = \alpha(\hat{\eta}, y, t), \tag{3}$$

is called an observer for the system (1)-(2), if there exist mappings

$$\beta : \mathbb{R}^p \times \mathbb{R}^m \times \mathbb{R} \to \mathbb{R}^p,$$

$$\phi : \mathbb{R}^n \to \mathbb{R}^p,$$

with ϕ left invertible, such that the manifold

$$\mathcal{M}_t = \{(\eta, y, \hat{\eta}) \in \mathbb{R}^n \times \mathbb{R}^m \times \mathbb{R}^p : \beta(\hat{\eta}, y, t) = \phi(\eta)\}, \tag{4}$$

has the following properties [16]:

1. All trajectories of the extended system (1)-(3) that start on the manifold $\mathcal{M}_t$ at time t remain there for all future times, $\tau > t$ i.e. $\mathcal{M}_t$ is positively invariant.

2. All trajectories of the extended system (1)-(3) that start in a neighborhood of $\mathcal{M}_t$ asymptotically converge to $\mathcal{M}_t$.

A mapping function $\Psi(x, y, t) : \mathbb{R}^l \times \mathbb{R}^m \times \mathbb{R} \to \mathbb{R}^p$ is left invertible with respect to x, if there exists another mapping $\Psi^L : \mathbb{R}^p \times \mathbb{R}^m \times \mathbb{R} \to \mathbb{R}^l$ such that $\Psi^L(\Psi(x, y, t), y, t) = x$ for all $x \in \mathbb{R}^l$ and for all y, t.

So from the definition of left invertibility, the estimate of η is given by $\phi^L(\phi(\eta))$ and the estimate on the manifold is given by $\phi^L(\beta(\hat{\eta}, y, t))$, as the estimation error $\hat{\eta} - \eta$ is zero on the manifold.

The mapping function β should be chosen such that (A1) holds:

(A1) $\det\left(\dfrac{\partial \beta}{\partial \hat{\eta}}\right) \neq 0$.

(A2) As off-the-manifold trajectories are given as

$$z = \beta(\hat{\eta}, y, t) - \phi(\eta), \tag{5}$$

the z dynamics are then given as

$$\dot{z} = \frac{\partial \beta}{\partial \hat{\eta}}\alpha(\hat{\eta}, y, t) + \frac{\partial \beta}{\partial y}h(\eta, y, t) + \frac{\partial \beta}{\partial t} - \frac{\partial \phi}{\partial \eta}f(\eta, y, t). \tag{6}$$

On the manifold, z and $\dot{z}$ will converge to zero and then the function $\alpha(\hat{\eta}, y, t)$ will be an observer for the system (1)-(2), given by

$$\alpha(\hat{\eta}, y, t) = \left(\frac{\partial \beta}{\partial \hat{\eta}}\right)^{-1}\left(-\frac{\partial \beta}{\partial y}h(\phi^L(\beta(\hat{\eta}, y, t)), y, t) - \frac{\partial \beta}{\partial t} + \frac{\partial \phi}{\partial \eta}\bigg|_{\eta = \phi^L(\beta(\hat{\eta}, y, t))} f(\phi^L(\beta(\hat{\eta}, y, t)), y, t)\right). \tag{7}$$

For dynamics that are not on the manifold (i.e. $z \neq 0$), then substituting the function $\alpha(\hat{\eta}, y, t)$ from (7) in (6) and making sure that (A1) holds, gives

$$\dot{z} = \frac{\partial \beta}{\partial y}\left(h(\eta, y, t) - h(\phi^L(\phi(\eta) + z), y, t)\right) - \frac{\partial \phi}{\partial \eta}f(\eta, y, t) + \frac{\partial \phi}{\partial \eta}\bigg|_{\eta = \phi^L(\phi(\eta) + z)} f(\phi^L(\phi(\eta) + z), y, t). \tag{8}$$

The mapping functions should be selected in such a way that (7) has a (locally) asymptotically stable equilibrium at $z = 0$, uniformly in η, y, t , where ϕ^L is left inverse of ϕ and z is the distance between system trajectories and the manifold.

It can be seen from (7) that (A1) should hold for the existence of function $\alpha(\hat{\eta}, y, t)$. (A2) should hold for the asymptotic convergence of off-the-manifold trajectories towards the manifold and to ensure that the distance z converges to zero. The function $\alpha(y, \hat{\eta}, t)$ renders the manifold invariant and (A2) makes the manifold attractive. So the problem of observer design has been reduced into making the $\dot{z}$ dynamics asymptotically stable.

3. 2-DOF Nonlinear Spring Damper System

The example system under consideration in this paper is the multi-input multi-output (MIMO) two degree-of-freedom (2-DOF) nonlinear spring damper system shown in Fig. 1. A weak non-linearity is included in the system to represent large deflections that typically occur in a flexible structure. The system is subjected to a excitation signal, U_d, that creates unwanted vibrations of the two masses. To simulate the situation in flexible structures that suffer from unwanted vibrations, the damping constant, C_1, is chosen such that the two degree-of-freedom system is under-damped. As a result the open-loop system has two lightly damped resonances.

The equation of motion for the two degree-of-freedom system is given by Eq. (9) where X_1 and X_2 represent the displacement of mass m_1 and m_2 respectively, f_a represents the active actuator force, f_{sa} represents the semi-active actuator (MR damper) force, K_1, K_2 are the linear spring stiffnesses, K_3 is the nonlinear spring stiffness, C_1 is the damping coefficient and U_d is excitation signal.

$$
\begin{bmatrix} m_1 & 0 \\ 0 & m_2 \end{bmatrix} \begin{bmatrix} \ddot{X}_1 \\ \ddot{X}_2 \end{bmatrix} + \begin{bmatrix} C_1 & 0 \\ 0 & 0 \end{bmatrix} \begin{bmatrix} \dot{X}_1 \\ \dot{X}_2 \end{bmatrix} + \begin{bmatrix} K_1 + K_2 & -K_2 \\ -K_2 & K_2 \end{bmatrix} \begin{bmatrix} X_1 \\ X_2 \end{bmatrix} = \begin{bmatrix} -K_3 \\ 0 \end{bmatrix} X_1^3
$$
$$
+ \begin{bmatrix} f_a - f_{sa} \\ f_{sa} - U_d \end{bmatrix}. \tag{9}
$$

The system can be represented in state space form as

$$
\dot{x} = \begin{bmatrix} x_2 \\ \dfrac{1}{m_1}\Big(f_a - f_{sa} - K_1 x_1 - C_1 x_2 - K_2(x_1 - x_3) \\ -K_3 x_1^3\Big) \\ x_4 \\ \dfrac{1}{m_2}\Big(f_{sa} - K_2(x_3 - x_1) - U_d\Big) \end{bmatrix}, \tag{10}
$$

where x_1 and x_2 are the unknown states representing the displacement and velocity of mass m_1 respectively; x_3 and x_4 are the known states representing the displacement and velocity of mass m_2 respectively.
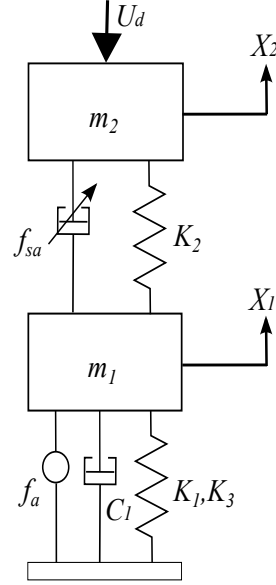
Figure 1: *2-DOF mass-spring-damper system, where f_a represents the force of an active actuator and f_{sa} represents the force of a semi-active device (MR damper). m_1, m_2 represent the masses, K_1, K_2 are the linear spring stiffness, K_3 is the nonlinear spring stiffness, C_1 is the damping coefficient and U_d is external disturbance signal.*

The controller for the 2-DOF system is based on a hybrid active and semi-active control methodology which combines an active actuator and semi-active device. The active actuator is designed to assist the semi-active device to achieve as close to fully active control performance as possible. The purpose is to design an observer that will operate effectively for this closed loop system. More specifically, an observer that can estimate the displacement and velocity for one of the two degrees-of-freedom is a suitable solution in this case.

4. Proposed Observer Design for the Example System

Following the observer design methodology presented in Section 2, the mapping functions $\phi(x_1, x_2)$ and $\beta\left(\hat{\eta}, x_3, x_4\right)$ can be defined as

$$\phi(x_1, x_2) = \begin{bmatrix} x_1 \\ x_2 \\ K_3 x_1^3 \end{bmatrix}, \quad \beta\left(\hat{\eta}, x_3, x_4\right) = \begin{bmatrix} \beta_1\left(\hat{\eta}, x_3, x_4\right) \\ \beta_2\left(\hat{\eta}, x_3, x_4\right) \\ \beta_3\left(\hat{\eta}, x_3, x_4\right) \end{bmatrix}, \tag{11}$$

The mapping $\phi(x_1, x_2)$ is defined in terms of the unknown states, in such a way that the rank of the matrix is equal to the number of rows, hence the condition of left invertability is satisfied. The mapping $\beta\left(\hat{\eta}, x_3, x_4\right)$ is defined in terms of the known states and the observer states.

Here z represents the distance between system trajectories and the manifold, such that

$$z = \beta\left(\hat{\eta}, x_3, x_4\right) - \phi(x_1, x_2). \tag{12}$$

The error dynamics are then given as

$$\dot{z} = \frac{\partial \beta}{\partial \hat{\eta}} \dot{\hat{\eta}} + \frac{\partial \beta}{\partial x_3} \dot{x}_3 + \frac{\partial \beta}{\partial x_4} \dot{x}_4 - \dot{\phi}(x_1, x_2), \tag{13}$$

which becomes

$$\dot{z} = \frac{\partial \beta}{\partial \hat{\eta}} \dot{\hat{\eta}} + \frac{\partial \beta}{\partial x_3} x_4 + \frac{\partial \beta}{\partial x_4} \frac{1}{m_2} \Big(f_{sa} - K_2(x_3 - x_1) \Big) - \begin{bmatrix} x_2 & \dot{x}_2 & 3K_3 x_1^2 x_2 \end{bmatrix}^{\mathsf{T}}, \tag{14}$$

leading to

$$\dot{z} = \frac{\partial \beta}{\partial \hat{\eta}} \dot{\hat{\eta}} + \frac{\partial \beta}{\partial x_3} x_4 + \frac{\partial \beta}{\partial x_4} \frac{1}{m_2} \Big(f_{sa} - K_2(x_3 - (\beta_1 - z_1)) \Big) - $$
$$\begin{bmatrix} \beta_2 - z_2 \\\\ \frac{1}{m_1} \Big(f_a - f_{sa} - K_1(\beta_1 - z_1) - C_1(\beta_2 - z_2) - K_2(\beta_1 - z_1 - x_3) - \\ (\beta_3 - z_3) \Big) \\\\ 3K_3(\beta_1 - z_1)^2(\beta_2 - z_2) \end{bmatrix}. \tag{15}$$

If the $\beta\,(\hat{\eta}, x_3, x_4)$ mapping function is selected in such a way that (A1) holds then the observer dynamics can be selected as in (7) to give

$$\dot{\hat{\eta}} = \left(\frac{\partial \beta}{\partial \hat{\eta}} \right)^{-1} \left(-\frac{\partial \beta}{\partial x_3} x_4 - \frac{\partial \beta}{\partial x_4} \frac{1}{m_2} \Big(f_{sa} - K_2(x_3 - \beta_1) \Big) \right) +$$
$$\left(\frac{\partial \boldsymbol{\beta}}{\partial \hat{\boldsymbol{\eta}}} \right)^{-1} \begin{bmatrix} \beta_2 \\\\ \frac{1}{m_1} \Big(f_a - f_{sa} - K_1\beta_1 - C_1\beta_2 - K_2(\beta_1 - x_3) - \beta_3 \Big) \\\\ 3K_3\beta_1^2\beta_2 \end{bmatrix}. \tag{16}$$

Then the error dynamics becomes

$$\dot{z} = \frac{\partial \beta}{\partial x_4} \frac{1}{m_2} \Big(-K_2 z_1 - C_2 z_2 \Big) - \begin{bmatrix} -z_2 \\\\ \frac{1}{m_1} \Big((K_1 + K_2)z_1 + C_1 z_2 + C_2 z_2 + z_3 \Big) \\\\ -3K_3 x_1^2 z_2 \end{bmatrix}. \tag{17}$$

Now the mapping function $\beta\,(\hat{\eta}, x_3, x_4)$ needs to be selected in such a way that (A1) and (A2) are satisfied. The $\beta\,(\hat{\eta}, x_3, x_4)$ mapping function is selected as

$$\beta\,(\hat{\eta}, x_4) = \begin{bmatrix} \hat{\eta}_1 & \hat{\eta}_2 & \hat{\eta}_3 + \dfrac{3K_3 m_2 \alpha x_4}{C_2} \end{bmatrix}^{\mathsf{T}}, \tag{18}$$

where α is a constant.

1. The first condition that needs to be satisfied by the $\beta\left(\hat{\eta}, x_4\right)$ mapping function is $\det\left(\dfrac{\partial\beta}{\partial\hat{\eta}}\right) \neq 0$. For the function given in (18) we have

$$\det\left(\frac{\partial\beta}{\partial\hat{\eta}}\right) = 1.$$

Therefore the first condition is satisfied.

2. The second condition is that the error dynamics

$$\dot{z} = \begin{bmatrix} z_2 \\ -\dfrac{1}{m_1}\Big((K_1 + K_2)z_1 + (C_1 + C_2)z_2 + z_3\Big) \\ -\dfrac{3K_2 K_3 \alpha z_1}{C_2} - 3K_3 \alpha z_2 + 3K_3 x_1^2 z_2 \end{bmatrix}, \tag{19}$$

should have an asymptotically stable equilibrium at $z = 0$. As the error dynamics are nonlinear, Lyapunov's second method is utilized to analyze stability and the Lyapunov function candidate (20) is used.

$$V(z) = \frac{1}{2}\left(z_1^2 + z_2^2 + z_3^2\right), \tag{20}$$

As

$$V(0) = 0, \tag{21a}$$

$$V(z) > 0, \quad \text{in } D - \{0\}, \tag{21b}$$

$$V(z) \ \text{ is radially unbounded}, \tag{21c}$$

Then

$$\dot{V}(z) = -\left(\frac{C_1 + C_2}{m_1}\right)z_2^2 - \left(\frac{K_1 + K_2}{m_1} - 1\right)|z_1||z_2| - \left(\frac{3K_2 K_3 \alpha}{C_2}\right)|z_1||z_3| - \left(3K_3\alpha + \frac{1}{m_1}\right)$$
$$|z_2||z_3| < 0,$$

$$\dot{V}(z) < 0, \quad \text{in } D - \{0\}. \tag{21d}$$

hence the equilibrium point $z = 0$ is global asymptotic stability, where D is the subset of $\mathbb{R}^p$ in which the Lyapunov function is defined.

In the next section the proposed observer is compared with an observer based on Lipschitz type nonlinearity.

5. Observer Design Based on Lipschitz Type Non-linearity

For comparison purposes a nonlinear observer based on the solution of the Riccati equation is designed for the system under consideration. This method is very well known for the class of systems that have Lipschitz type non-linearity. The example system in this paper has a cubic stiffness, which is locally Lipschitz but there is a limit on its growth due to the mechanical constraint, which makes it globally Lipschitz. Consider a system of the form

$$\dot{x} = Ax + g(t, u, y) + f(t, u, x), \tag{22}$$

$$y = Cx,$$

where $x \in \mathbb{R}^v$ is the system state, $y \in \mathbb{R}^m$ is the system measurable output, $u \in \mathbb{R}^z$ is the input, A and C are constant matrices, $g : \mathbb{R} \times \mathbb{R}^z \times \mathbb{R}^m \to \mathbb{R}^v$, $f : \mathbb{R} \times \mathbb{R}^z \times \mathbb{R}^v \to \mathbb{R}^v$, and an over-dot represents the differentiation with respect to time. The nonlinear function $f(t, u, x)$ is assumed to be globally Lipschitz in x with a Lipschitz constant γ. A and C are assumed to be observable. For the system in (22) the observer is defined as

$$\dot{\hat{x}} = A\hat{x} + g(t, u, y) + f(t, u, \hat{x}) + L(y - C\hat{x}), \tag{23}$$

where $\hat{x}$ represents the observer state, $L \in \mathbb{R}^{n \times q}$ is the observer gain matrix. The error dynamics are represented as

$$\dot{\tilde{x}} = (A - LC)\tilde{x} + f(t, u, x) + f(t, u, \hat{x}), \tag{24}$$

where $\tilde{x} = x - \hat{x}$. Now the algorithm below presents a method to choose L which will make the error dynamics stable

1. Set ϵ to a positive value.

2. Solve the following Algebraic Riccati Equation (ARE)

$$AP + PA^\mathsf{T} + P\left(\gamma^2 I - \frac{1}{\epsilon}C^\mathsf{T}C\right)P + I + \epsilon I = 0. \tag{25}$$

3. If P is symmetric and positive definite, then setting

$$L = (\frac{1}{2\epsilon})PC^\mathsf{T}, \tag{26}$$

in (23) gives stable error dynamics (24).

4. If not, set $\epsilon = \dfrac{\epsilon}{2}$ and go to step 2. If ϵ is below some precision value, abandon method.

The 2-DOF mass-spring-damper system (10) can be represented by (27)

$$\dot{x} = Ax + f(x) + g(y)u, \tag{27}$$

where

$$A = \begin{bmatrix} 0 & 1 & 0 & 0 \\ -\dfrac{(K_1 + K_2)}{m_1} & -\dfrac{(C_1 + C_2)}{m_1} & \dfrac{K_2}{m_1} & \dfrac{C_2}{m_1} \\ 0 & 0 & 0 & 1 \\ \dfrac{K_2}{m_2} & 0 & -\dfrac{K_2}{m_2} & 0 \end{bmatrix}, \quad g = \begin{bmatrix} 0 & 0 \\ \dfrac{1}{m_1} & -\dfrac{1}{m_1} \\ 0 & 0 \\ 0 & \dfrac{1}{m_2} \end{bmatrix}, \quad f = \begin{bmatrix} 0 \\ 0 \\ 0 \\ -K_3 x_1^3 \end{bmatrix}, \quad C = \begin{bmatrix} 0 & 0 \\ 0 & 0 \\ 1 & 0 \\ 0 & 1 \end{bmatrix}^\mathsf{T}.$$

The Lipschitz constant is required to solve the Riccati equation (25). A function $f(x)$ is said to be globally Lipschitz if there exists a constant γ such that for all $x_a, x_b \in \mathbb{R}^n$, the following holds,

$$|f(x_a) - f(x_b)| \leq \gamma |x_a - x_b|. \tag{28}$$

To find the Lipschitz constant for the system under consideration, (28) is used as

$$|f(x_{1a}) - f(x_{1b})| \leq |K_3 x_{1a}^3 - K_3 x_{1b}^3|,$$

$$|f(x_{1a}) - f(x_{1b})| \leq \gamma |x_{1a} - x_{1b}|. \tag{29}$$

Where $\gamma = |K_3||x_{1a}^2 + x_{1a} x_{1a} + x_{1b}^2|$. As there is a constraint on $x_1 \leq 27.5 \ mm$ because of the mechanical design, this puts a saturation limit on the amplitude of non-linearity and makes the system globally Lipschitz. The Lipschitz constant $\gamma = 7.56$ is computed using (29).

To compute the observer gain matrix L, the algorithm described in the same section is used, ϵ is set to 1 and P is computed by solving the Riccati equation given in (25) using Matlab.

$$P = \begin{bmatrix} 2.6699 & -0.1297 & -0.7979 & 0.0098 \\ -0.1297 & 0.0189 & -0.0039 & 0.0101 \\ -0.7979 & -0.0039 & 2.0582 & -0.1985 \\ 0.0098 & 0.0101 & -0.1985 & 0.0477 \end{bmatrix}. \tag{30}$$

P is symmetric and positive definite, hence L is computed using (26), and the result is that

$$L = \begin{bmatrix} -0.3990 & -0.0020 & 1.0291 & -0.0993 \\ 0.0049 & 0.0051 & -0.0993 & 0.0238 \end{bmatrix}^\mathsf{T}. \tag{31}$$

6. Simulation Results

After designing observers for the 2-DOF mass-spring-damper system using the proposed technique and the method based on Lipschitz type non-linearity, simulations were carried out using Matlab/Simulink to check the performance

Table 1: System parameters

mass (kg)	stiffness (Nm^{-1})	damping (Nsm^{-1})
$m_1 = 100$	$K_1 = 100000$	$C_1 = 1000$
$m_2 = 112$	$K_2 = 63000$	$C_2 = 1000$

of both the observers under different conditions. The system is excited by introducing the sinusoidal signal U_d at mass m_2 as shown in Fig. 1 with an amplitude of 70 N at 3 Hz. The resonant frequencies of the 2-DOF system are 2.76 Hz and 6.8 Hz. The observer is designed for a closed loop system with a hybrid controller to control vibrations in a system with natural frequencies below 10 Hz. So the parameters are chosen accordingly. Table 1 shows the parameters of the 2-DOF system.

Fig. 2 shows the actual and estimated displacement and velocity of mass m_1 under different conditions. Under normal conditions, i.e. without any parameter variation or any phase change in the excitation signal, the performance of both observers is satisfactory as shown in Fig. 2a. In Fig. 2b delay has been added to the phase of the excitation signal and the performance of the proposed observer is better than the observer based on Lipschitz type non-linearity. Fig. 2c shows the same signals but with the system parameters varied. Both the masses m_1 and m_2 are increased by 25% and again the proposed observer is performing better. To check the performance of both the observers against measurement noise, Gaussian noise is added to the acceleration of mass m_2 as shown in Fig. 3a. Both the observers are estimating well, but at some points the proposed observer performance is better, as shown in Fig. 4a. Now the Gaussian noise is added to the displacement of mass m_2 as shown in Fig. 3b. In this case again the performance of the proposed observer is impressive, whereas on the other hand the observer based on Lipschitz type nonlinearity is not performing well as shown in Fig. 4b.

To further check the robustness of both the observers against different disturbances which includes a ramp, step, sinusoidal and random signals are used. Fig. 5a and Fig. 5b shows the performance of both the observers against step and ramp disturbance signals respectively, introduced at mass m_2 starting at one second and ends at two second. Again the proposed observer out-performed the others. In Fig. 6a and Fig. 6b a sinusoidal disturbance of 1 Hz and 100 Hz is introduced at mass m_2 respectively. At low frequency sinusoidal disturbance the proposed observer is performing better whereas at high frequency sinusoidal disturbance both the observers are performing well. In Fig. 7 a random disturbance is introduced at mass m_2, and again the proposed observer estimation is quite good as compared to the observer based on Lipschitz type nonlinearity. In Fig. 8 different initial conditions are given to the actual system. The converging rate of the proposed observer is faster. Robustness of the observer is an important aspect, especially when it needs to be used in the closed loop control system. The examples shown here demonstrate the potential of the proposed observer in terms of robustness to both parameter variation and phase change in the excitation signal.
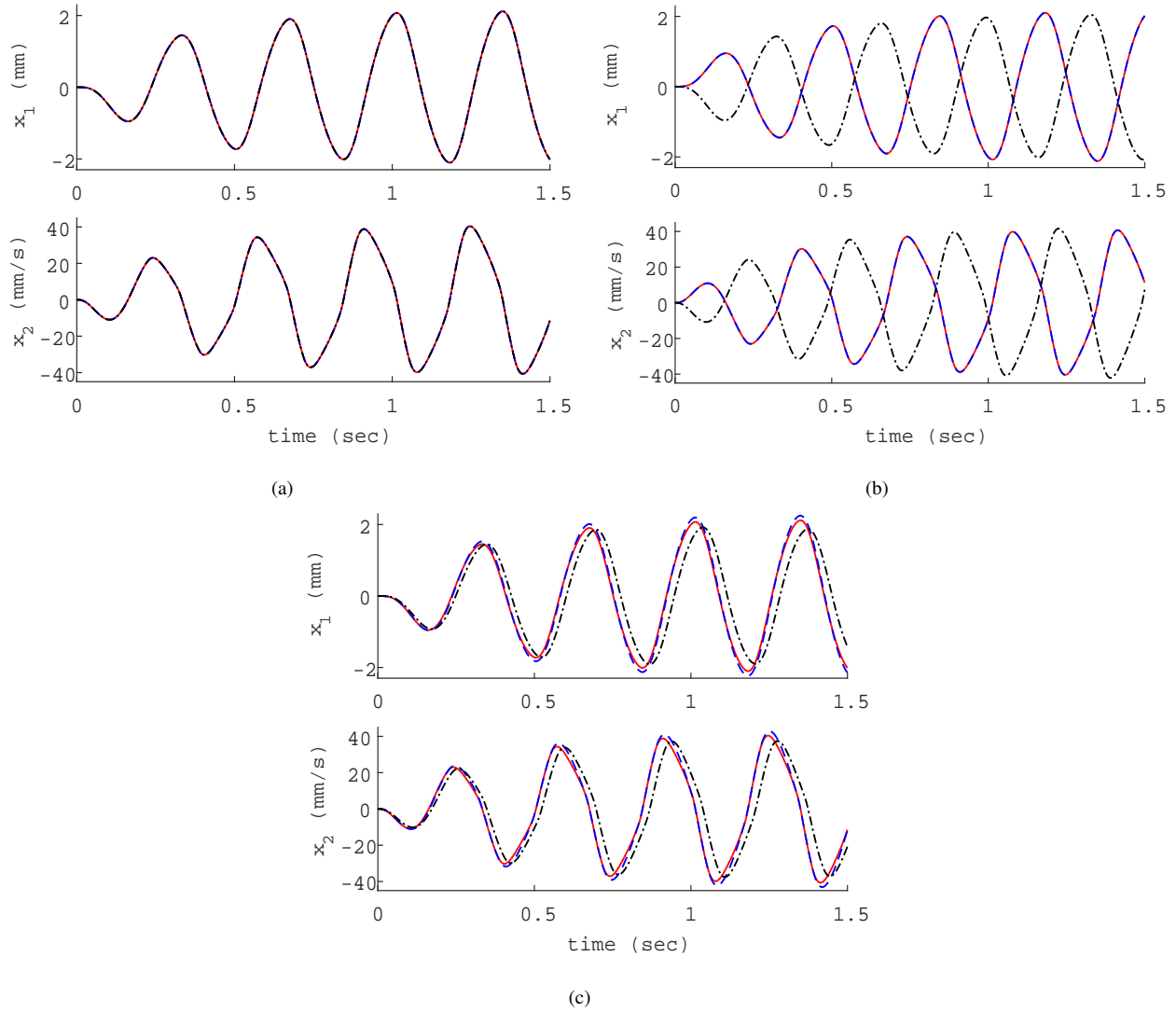
Figure 2: *Simulated actual and estimated displacement and velocity of mass m_1. The solid line represents actual measurements, dashed line represents the estimated measurements using the proposed observer, dash-dot line represents the estimated measurements using the observer based on Lipschitz type non-linearity, (a) under normal conditions, (b) with phase delay in the excitation signal, (c) with 25% increase in both the masses.*
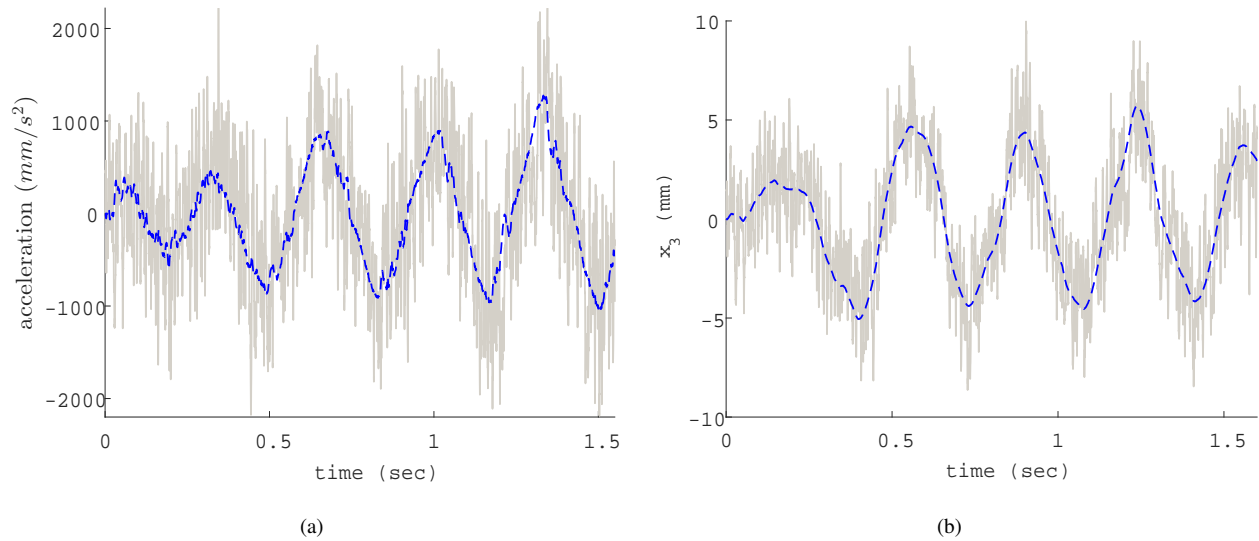
Figure 3: *Acceleration and displacement of mass m_2 with and without Gaussian noise. The dashed line represents the signal without Gaussian noise, solid line represents the signal with Gaussian noise, (a) Gaussian noise is added to the acceleration of mass m_2, (b) Gaussian noise is added to the displacement of mass m_2.*
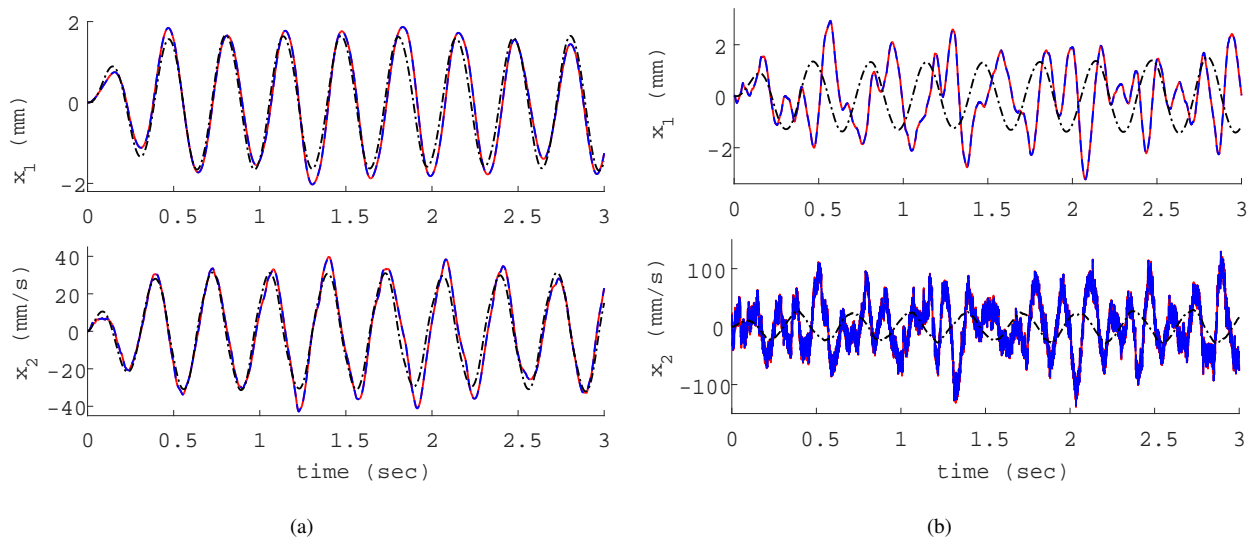

Figure 4: *Simulated actual and estimated displacement and velocity of mass m_1 with measurement noise (Gaussian noise). The solid line represents actual measurements, dashed line represents the estimated measurements using the proposed observer, dash-dot line represents the estimated measurements using the observer based on Lipschitz type non-linearity, (a) Gaussian noise is added to the acceleration of mass m_2, (b) Gaussian noise is added to the displacement of mass m_2.*
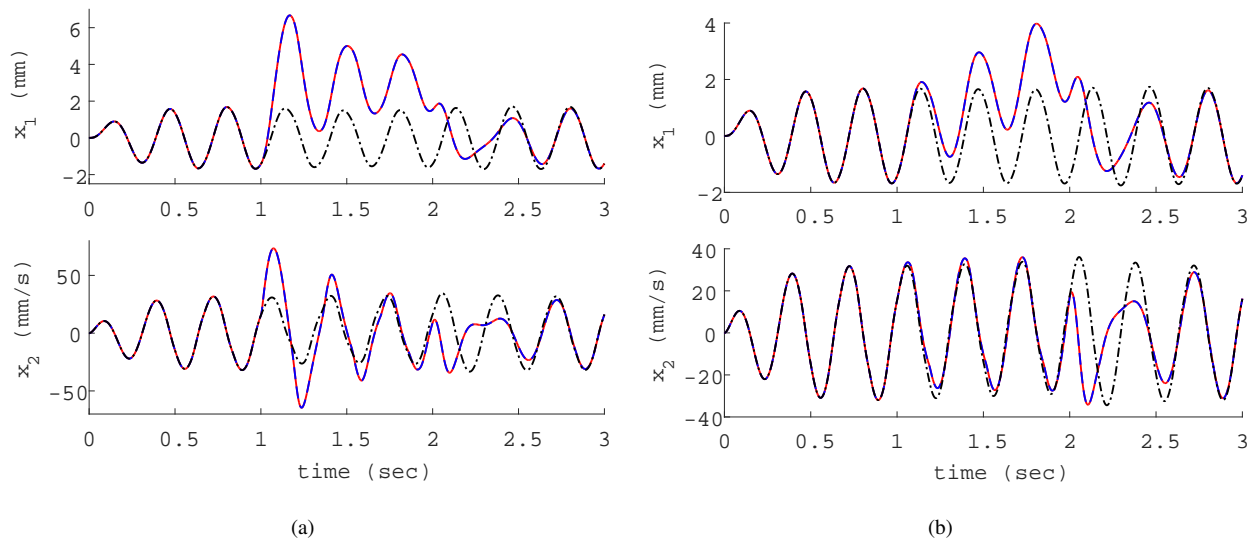
Figure 5: *Simulated actual and estimated displacement and velocity of mass m_1 with step and ramp disturbance signals introduced at mass m_2. The solid line represents actual measurements, dashed line represents the estimated measurements using the proposed observer, dash-dot line represents the estimated measurements using the observer based on Lipschitz type non-linearity, (a) with step disturbance signal, (b) with ramp disturbance signal.*
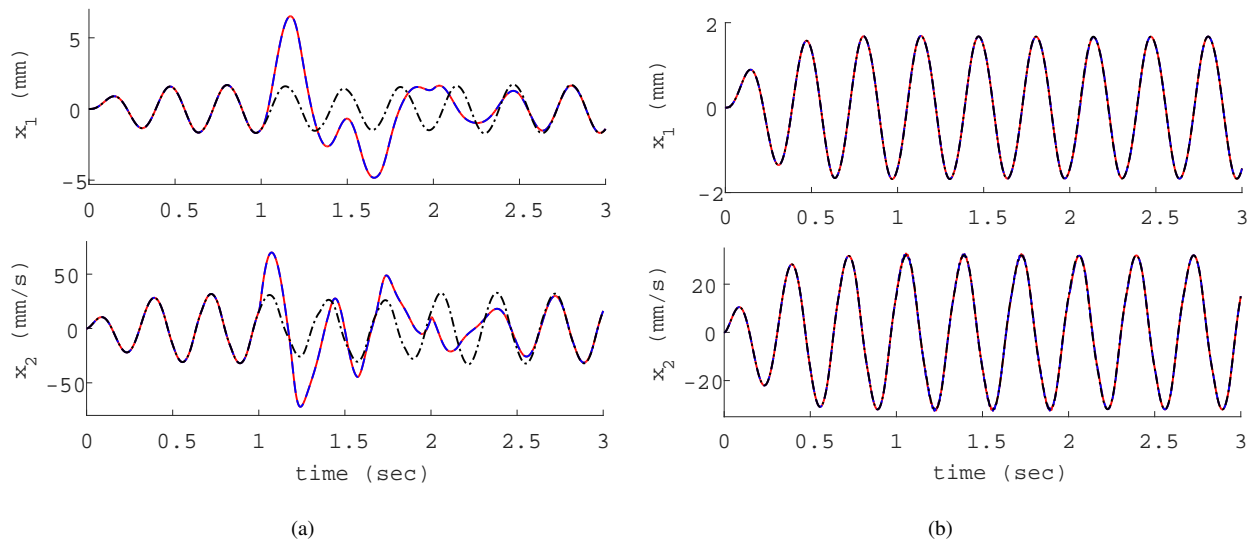

Figure 6: *Simulated actual and estimated displacement and velocity of mass m_1 with sinusoidal disturbance signal at mass m_2. The solid line represents actual measurements, dashed line represents the estimated measurements using the proposed observer, dash-dot line represents the estimated measurements using the observer based on Lipschitz type non-linearity, (a) with sinusoidal disturbance of 1 Hz, (b) with sinusoidal disturbance of 100 Hz.*
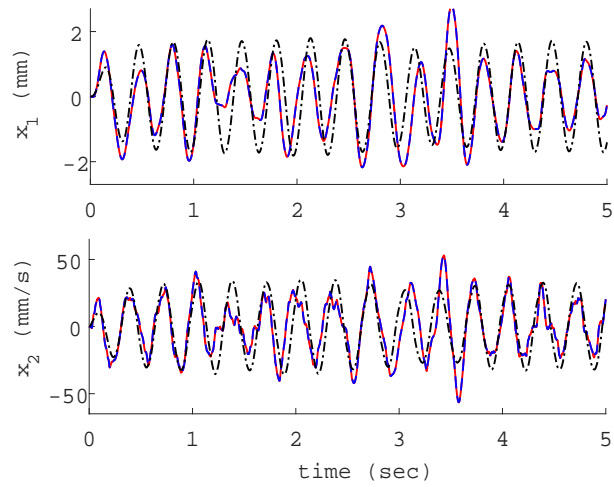
Figure 7: *Simulated actual and estimated displacement and velocity of mass m_1 with random disturbance signal at mass m_2. The solid line represents actual measurements, dashed line represents the estimated measurements using the proposed observer, dash-dot line represents the estimated measurements using the observer based on Lipschitz type non-linearity.*

Figure 8: *Simulated actual and estimated displacement and velocity of mass m_1 with different initial conditions. The solid line represents actual measurements, dashed line represents the estimated measurements using the proposed observer, dash-dot line represents the estimated measurements using the observer based on Lipschitz type non-linearity.*
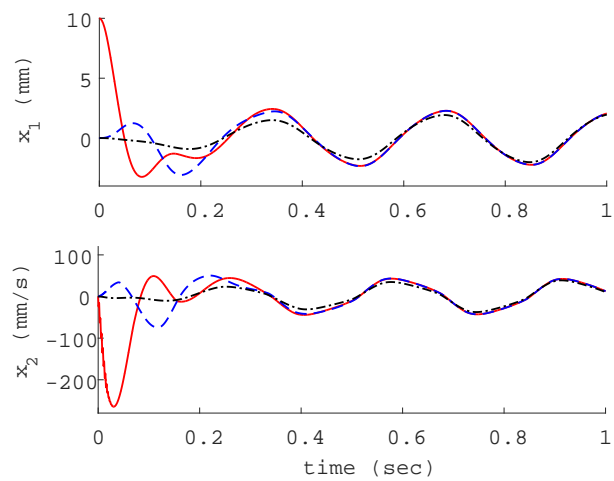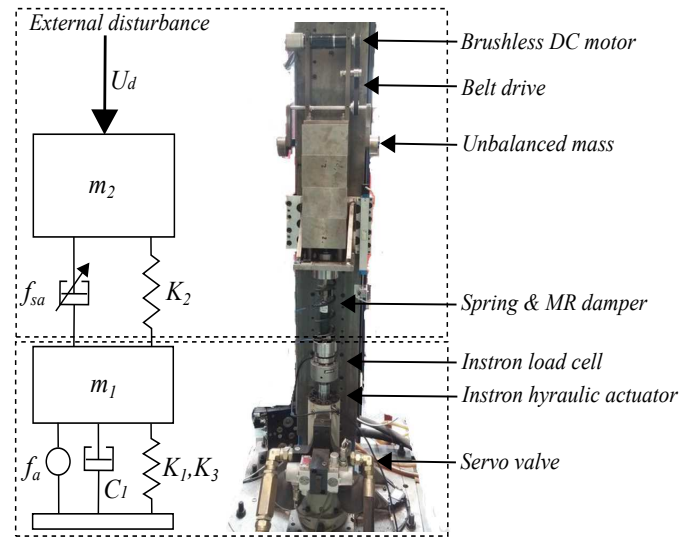
Figure 9: *Hardware in loop (HIL) test set-up, where f_a represents the force of an active actuator and f_{sa} represents the force of a semi-active actuator (MR damper). m_1, m_2 represent the masses, K_1, K_2 are the liner spring stiffness, K_3 is the nonlinear spring stiffness, C_1 is the damping coefficient.*

7. Experimental Results

The experimental tests are performed as hardware-in-the-loop (HIL) tests. The experimental system is shown in Fig. 9, and details on the experimental facility are given in [38]. The physical part of the HIL test is the degree-of-freedom that includes mass m_2, the MR damper and the linear spring. The other degree-of-freedom that includes the mass m_1, the active actuator, linear damper C_1 and nonlinear spring is the non-physical part of the HIL test. This is simulated numerically and applied to the physical system via a force applied by an Instron hydraulic actuator.

The displacement of mass m_1 from Simulink goes into the Instron 8400 controller via a National Instruments data acquisition card. The control signal from the Instron 8400 controller is applied to the Instron hydraulic actuator via servo valves and the LVDT gives the feedback displacement signal.

In the experimental test, the excitation signal is generated by rotating unbalanced masses driven by a brush-less DC motor, whose speed is controlled through a separate motor speed controller. The speed controller keeps the speed of the motor close to the desired speed but there is a small amount of variation, so it is not a perfect single frequency sine wave, and the phase is also unknown. Fig. 10 shows the actual and estimated displacement and velocity of mass m_2 under three different conditions. As mentioned earlier, the phase of the excitation signal is not known, so after doing several trials, results were selected such that the phase of the excitation signal generated experimentally best matches the phase applied in the simulation results. In this case both the observers are estimating quite well as shown in Fig. 10a. In Fig. 10b the excitation signal has deliberately introduced phase delay and then in Fig. 10c both the masses m_1 and m_2 are increased by 25% in addition to the phase delay. In both cases the proposed observer continues to perform well, which experimentally validates the simulation results. It also adds further evidence of the potential for
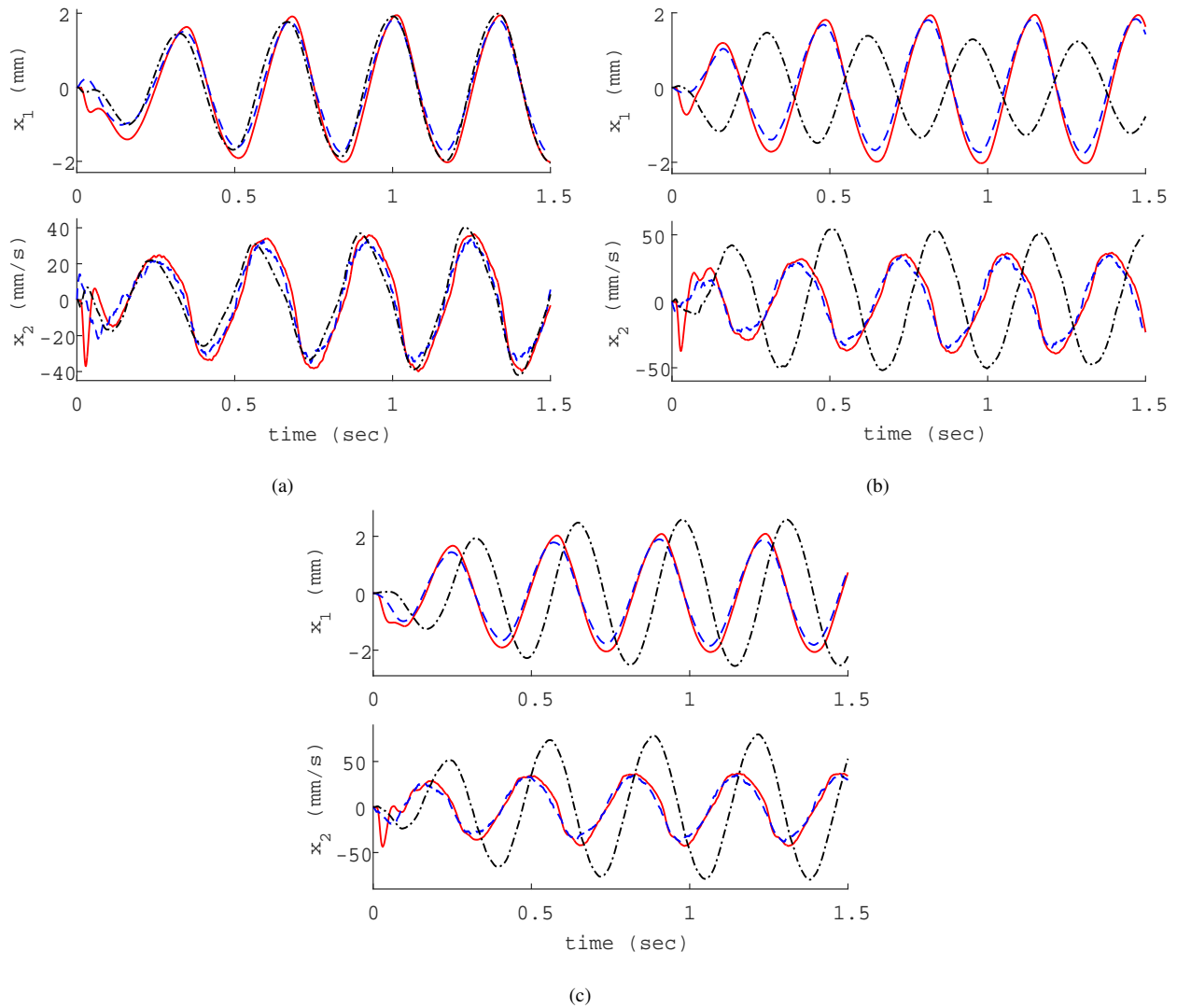
Figure 10: *Experimental actual and estimated displacement and velocity of mass m_1. The solid line represents actual measurements from the LVDT, dashed line represents the estimated measurements using the proposed observer, dash-dot line represents the estimated measurements using the observer based on Lipschitz type non-linearity, (a) under normal conditions, (b) with phase delay in the excitation signal, (c) with 25% increase in both the masses.*
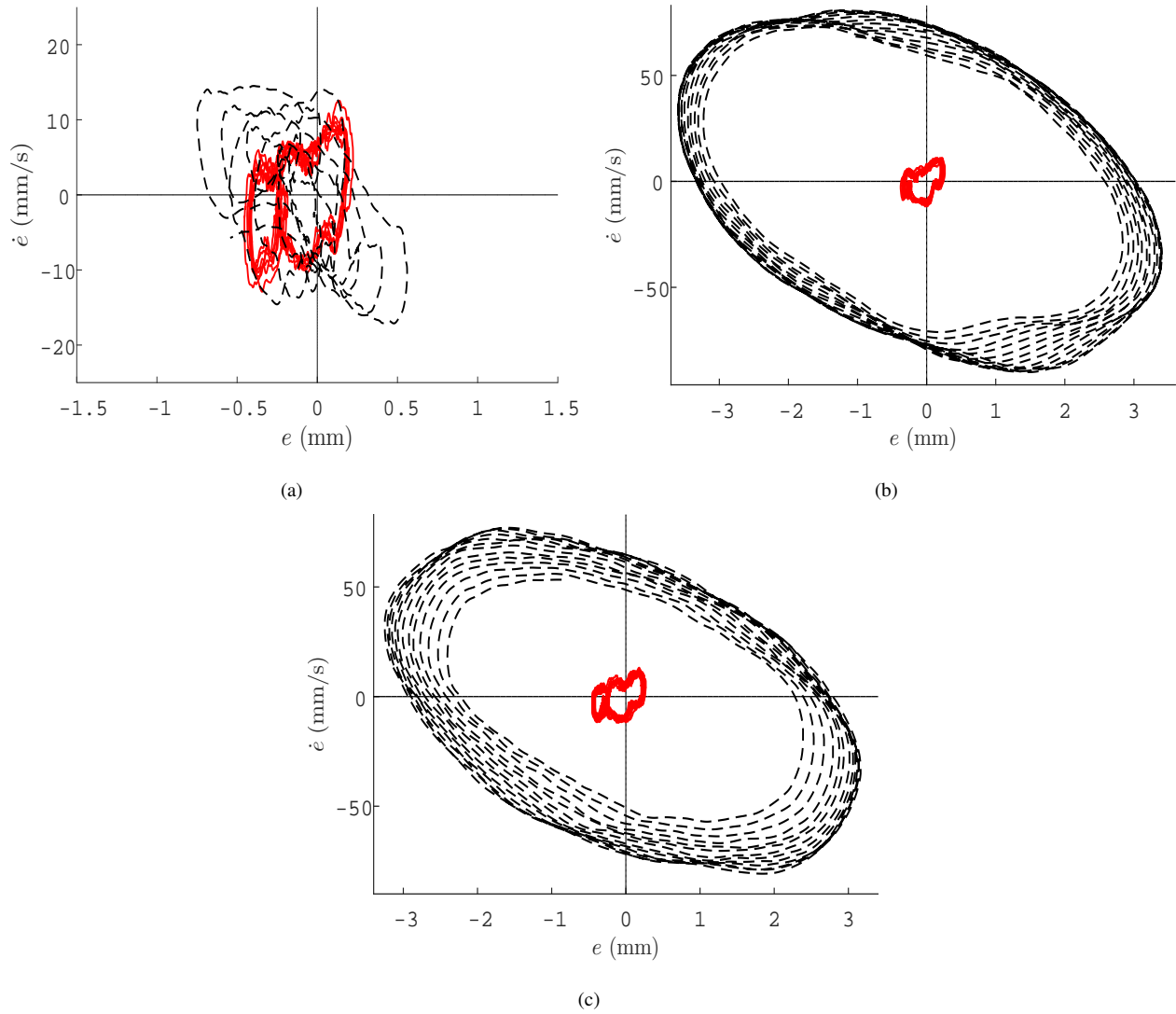
Figure 11: *Error dynamics in experiment, where the dashed line represents the error dynamics in the proposed observer and the dash-dot line represents the error dynamics in the observer based on Lipschitz type non-linearity, (a) under normal conditions, (b) with 25% increase in both the masses, (c) with phase delay in the disturbance signal.*

Table 2: Comparison of observers based on parameter variation (simulation)

System parameters (25% increase)	Proposed observer error (mm)	Lipschitz based observer error (mm)
m_1 & m_2	0.13	0.96
K_1 & K_2	0.18	1.04
C_1 & C_2	0.05	0.5

this observer for offering improved performance over existing observers.

For a quantitative analysis, a performance index is defined in terms of the absolute value of the radius of the phase planes shown in Fig. 11. This shows the deterioration in performance for both the observers, with the parameter variation and phase change in the excitation signal. The phase planes in Fig. 11 are plotted using experimental data. The error is increased from $0.5\ mm$ to $3\ mm$ for the observer based on Lipschitz type nonlinearity in both the scenarios as shown in Figs. 11b and 11c, but for the proposed observer, the error remains almost the same in all the cases. To further check the robustness of both the observers to parameter variation, a comparison is summarized in Table 2. Simulation results are used in order to investigate a broader range of parameter variations. It can be concluded that the proposed observer is robust to both parameter variation and phase change in the excitation signal for the range and type of parameters considered in this study.

The final step is to check the performance of the proposed observer as part of a closed loop control system in the experimental setup. The controller uses a hybrid combination of a semi-active device and an active control actuator to suppress vibrations. The control framework used is the immersion and invariance (I & I) control technique in combination with sliding mode control (SMC). I & I is used to design the controller for the active actuator and SMC is used to design the controller for the semi-active actuator using the same target/reference system. A full description of the details of the hybrid active and semi-active control algorithm are beyond the scope of the present contribution. However, Fig. 12 shows the actual and estimated displacement and velocity of mass m_1 in the closed loop system. The results show very good agreement.

8. Conclusion

One of the major issues with nonlinear observers is that most of them do not possess a structural design methodology and if they do, then some of the conditions are very difficult to meet. Secondly most of these methods are designed for a specific class of systems, like the one that is used for comparison purposes, it is only applicable to the systems that have Lipschitz type non-linearity and satisfies the globally Lipschitz conditions. The proposed observer is restricted to systems where an invariant manifold exists, and for such systems it provides a structured design methodology.
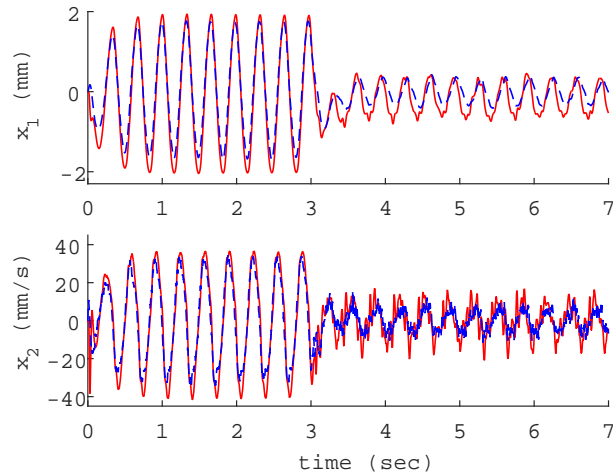
Figure 12: *Experimental actual and estimated displacement and velocity of mass m_1 with hybrid active and semi-active controller, where the solid line represents actual measurement from LVDT, dashed line represents the estimated measurement using the proposed observer. An Immersion and invariance (I&I) methodology is used to design the controller for active actuator [16] and sliding mode control (SMC) methodology is used for the semi-active controller [39]. Magneto-rheological (MR) damper is used as a semi-active actuator and hydraulic actuator is used as an active actuator.*

Robustness is a crucial property, especially when the observer needs to be used in a closed loop control system because performance of the controller depends on the estimated signals. A qualitative analysis has been performed based on the performance index defined in Section 7. It is shown that the proposed observer error remains almost the same with the parameter variation and phase change in the excitation signal, whereas there is an increase in the error in all the scenarios for the observer based on Lipschitz type non-linearity.

In this paper, a method to design a reduced order observer for a nonlinear system has been presented. A systematic design method for the observer has been explained in detail. Then the performance of the proposed observer was tested using a 2-DOF example system. As part of this process, the proposed observer was compared with a well known observer based on Lipschitz type non-linearity. Based on this comparison, we conclude that the new observer has a clear performance benefit, with significant potential to be extended to a wider range of nonlinear systems beyond the one considered here.

The proposed observer was shown to have a better performance for the parameters and inputs selected in the example of a 2-DOF system. In particular, the robustness of the proposed observer against parameter variation and excitation signal is shown to be better both in the simulation and the experiment. Finally the proposed observer was found to perform well when tested in a closed loop with a hybrid active and semi-active controller system.

Acknowledgment

References

[1] M. Zeitz, The extended luenberger observer for nonlinear systems, Systems & Control Letters 9 (2) (1987) 149–156.

[2] M. G. Price, G. Cook, Identification/observation using an extended luenberger observer, IEEE Transactions on Industrial Electronics IE-29 (4) (1982) 279–287. doi:10.1109/TIE.1982.356680.

[3] M. Boutayeb, D. Aubry, A strong tracking extended kalman observer for nonlinear discrete-time systems, IEEE Transactions on Automatic Control 44 (8) (1999) 1550–1556.

[4] P. Mercorelli, A two-stage augmented extended kalman filter as an observer for sensorless valve control in camless internal combustion engines, IEEE Transactions on Industrial Electronics, 59 (11) (2012) 4236–4247. doi:10.1109/TIE.2012.2192892.

[5] F. Thau, Observing the state of non-linear dynamic systems, International journal of control 17 (3) (1973) 471–479.

[6] S. R. Kou, D. L. Elliott, T. J. Tarn, Exponential observers for nonlinear dynamic systems, Information and control 29 (3) (1975) 204–216.

[7] P. Vaclavek, P. Blaha, Lyapunov-function-based flux and speed observer for ac induction motor sensorless control and parameters estimation, IEEE Transactions on Industrial Electronics 53 (1) (2005) 138–145. doi:10.1109/TIE.2005.862305.

[8] H. Chaoui, N. Golbon, I. Hmouz, R. Souissi, S. Tahar, Lyapunov-based adaptive state of charge and state of health estimation for lithium-ion batteries, IEEE Transactions on Industrial Electronics 62 (3) (2015) 1610–1618. doi:10.1109/TIE.2014.2341576.

[9] A. Nikoobin, R. Haghighi, Lyapunov-based nonlinear disturbance observer for serial n-link robot manipulators, Journal of Intelligent and Robotic Systems 55 (2-3) (2009) 135–153.

[10] C. Lageman, R. Mahony, J. Trumpf, State observers for invariant dynamics on a Lie group, in: 18th International Symposium on Mathematical Theory of Networks and Systems, 2008, p. 8.

[11] S. E. Talole, J. P. Kolhe, S. B. Phadke, Extended-state-observer-based control of flexible-joint system with experimental validation, IEEE Transactions on Industrial Electronics 57 (4) (2010) 1411–1419.

[12] S. Li, J. Yang, W.-H. Chen, X. Chen, Generalized extended state observer based control for systems with mismatched uncertainties, Industrial Electronics, IEEE Transactions on 59 (12) (2012) 4792–4802.

[13] Y. Huang, K. Xu, J. Han, J. Lam, Flight control design using extended state observer and non-smooth feedback, in: Proceedings of the IEEE Conference on Decision and Control, Vol. 1, 2001, pp. 223–228.

[14] D. Maithripala, J. M. Berg, W. Dayawansa, An intrinsic observer for a class of simple mechanical systems on a lie group, in: Proceedings of the American Control Conference, Vol. 2, IEEE, 2004, pp. 1546–1551.

[15] C. Lageman, J. Trumpf, R. Mahony, Gradient-like observers for invariant dynamics on a lie group, IEEE Transactions on Automatic Control 55 (2) (2010) 367–377.

[16] A. Astolfi, D. Karagiannis, R. Ortega, Nonlinear and adaptive control with applications, Springer Science & Business Media, 2007.

[17] C. Edwards, C. P. Tan, Sensor fault tolerant control using sliding mode observers, Control Engineering Practice 14 (8) (2006) 897–908.

[18] F. Nollet, T. Floquet, W. Perruquetti, Observer-based second order sliding mode control laws for stepper motors, Control Engineering Practice 16 (4) (2008) 429–443.

[19] W. Perruquetti, J.-P. Barbot, Sliding mode control in engineering, CRC Press, 2002.

[20] J.-J. Slotine, J. Hedrick, E. Misawa, On sliding observers for nonlinear systems, Journal of Dynamic Systems, Measurement, and Control 109 (3) (1987) 245–252.

[21] C. Edwards, S. K. Spurgeon, C. P. Tan, N. Patel, Sliding-mode observers, in: Mathematical methods for robust and nonlinear control, Springer, 2007, pp. 221–242.

[22] K. Kalsi, J. Lian, S. Hui, S. H. Zak, Sliding-mode observers for uncertain systems, in: American Control Conference, 2009. ACC'09., IEEE, 2009, pp. 1189–1194.

[23] L. Fridman, Y. Shtessel, C. Edwards, X.-G. Yan, Higher-order sliding-mode observer for state estimation and input reconstruction in nonlinear systems, International Journal of Robust and Nonlinear Control 18 (4-5) (2008) 399–412.

[24] L. Fridman, A. Levant, J. Davila, Observation of linear systems with unknown inputs via high-order sliding-modes, International Journal of Systems Science 38 (10) (2007) 773–791.

[25] T. Floquet, J.-P. Barbot, A canonical form for the design of unknown input sliding mode observers, in: Advances in variable structure and sliding mode control, Springer, 2006, pp. 271–292.

[26] B. Walcott, S. Zak, Observation of dynamical systems in the presence of bounded nonlinearities/uncertainties, in: 1986 25th IEEE Conference on Decision and Control, no. 25, 1986, pp. 961–966.

[27] S. Drakunov, V. Utkin, Sliding mode observers. tutorial, in: Decision and Control, 1995., Proceedings of the 34th IEEE Conference on, Vol. 4, IEEE, 1995, pp. 3376–3378.

[28] F. Zhu, Z. Han, A note on observers for lipschitz nonlinear systems, IEEE Transactions on Automatic Control 47 (10) (2002) 1751–1754.

[29] W. Zhang, H. Su, H. Wang, Z. Han, Full-order and reduced-order observers for one-sided lipschitz nonlinear systems using riccati equations, Communications in Nonlinear Science and Numerical Simulation 17 (12) (2012) 4968–4977.

[30] A. Zemouche, M. Boutayeb, G. I. Bara, Observers for a class of lipschitz systems with extension to h performance analysis, Systems & Control Letters 57 (1) (2008) 18–27.

[31] Q. P. Ha, H. Trinh, State and input simultaneous estimation for a class of nonlinear systems, Automatica 40 (10) (2004) 1779–1785.

[32] I. U. Khan, R. Dhaouadi, Nonlinear reduced order observer design for elastic drive systems using invariant manifolds, in: IEEE International Conference on Mechatronics (ICM), IEEE, 2015, pp. 58–63.

[33] F. Morbidi, G. L. Mariottini, D. Prattichizzo, Observer design via immersion and invariance for vision-based leader–follower formation control, Automatica 46 (1) (2010) 148–154.

[34] D. Karagiannis, D. Carnevale, A. Astolfi, Invariant manifold based reduced-order observer design for nonlinear systems, IEEE Transactions on Automatic Control 53 (11) (2008) 2602–2614.

[35] G. Besancon, A. Ticlea, An immersion-based observer design for rank-observable nonlinear systems, IEEE Transactions on Automatic Control 52 (1) (2007) 83–88.

[36] A. Astolfi, R. Ortega, A. Venkatraman, A globally exponentially convergent immersion and invariance speed observer for mechanical systems with non-holonomic constraints, Automatica 46 (1) (2010) 182–189.

[37] S. Raghavan, J. K. Hedrick, Observer design for a class of nonlinear systems, International Journal of Control 59 (2) (1994) 515–528.

[38] D. Batterbee, N. Sims, Hardware-in-the-loop simulation of magnetorheological dampers for vehicle suspension systems, Journal of Systems and Control Engineering, Part I: Proceedings of the Institution of Mechanical Engineers 221 (2) (2007) 265–278.

[39] K. D. Young, V. I. Utkin, U. Ozguner, A control engineer's guide to sliding mode control, IEEE Transactions on Control Systems Technology 7 (3) (1999) 328–342.